

Theoretical Studies on the Reaction Mechanism of Vapor-Phase methanol Photocatalytic Degradation

¹HUIMIN BI*, ¹FUYING YOU, ¹YAN LIU, ¹XINGQUAN CHAI AND ²LINGPENG MENG

^aDepartment of Chemistry, Handan College, Hebei Handan 056002, China.

^bHebei Normal University, Shijiazhuang, Hebei Province 050091, China.

binbi99@163.com*

(Received on 4th April 2012, accepted in revised form 15th June 2012)

Summary:The reaction mechanism of methanol photocatalytic degradation by nano-titanium dioxide (TiO₂) have been studied at the B3LYP/6-311++G (2df, pd) level, and reaction channels have been found. The geometries of all compounds were optimized, the results indicate that the intermediate products are HCOOH and H₂O, last products of reaction are CO₂ and H₂O. Intermediates, transition states and products were optimized and IRC calculations were carried out. The calculated results explain the conclusion of experiment successfully. From the view of bond length and analysis of energy, the changes of chemical bonds in the reactions are discussed, the potential energy of the reaction is low, which is helpful for the experiment of the methanol photocatalytic degradation over nano-TiO₂.

Keywords: Methanol, Photocatalysis degradation, Reaction mechanism, Transition state.

Introduction

As a air pollutants, methanol is mainly from vehicle exhaust and industrial emissions, it is very harmful to human health. It is a hot problem to solve the pollution of methanol [1-5]. Alcohols and other oxygenated compounds have high photochemical reactivity. The photocatalytic degradation of methanol at room temperature by catalyzer of nano-TiO₂ was studied recent years [6-13], However, the studies on the mechanism of the reaction process are less, the reports of quantum chemical calculations from molecular level is so few. In this study, the mechanism of methanol photocatalytic degradation in the nano-TiO₂ is discussed by the quantum chemistry, we discuss the intermediates, transition states and the possible reaction channels.

Results and Discussions

Stability Configurations and Reaction Channels

The results of our calculation indicate that the possible reaction channels in fig. 1 (By irradiation and catalyst of nano-TiO₂, the H₂O was oxidated to •OH).

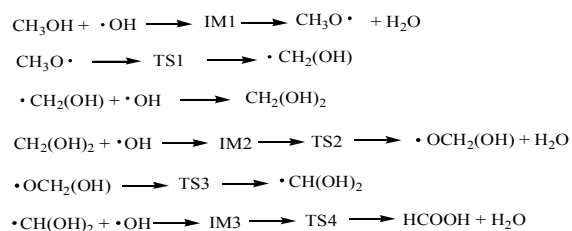


Fig. 1: The reaction channels.

Recently, the conclusion of our calculation show that [14], the products of carboxylic acid photocatalytic degradation in nano-TiO₂ surface are CO₂ and H₂O, therefore, the products of methanol photocatalytic degradation are CO₂ and H₂O too.

The geometry parameters of the reactants, products, potential intermediates, and transition states are shown in Fig. 2.

The frequencies are computed using the analytical second derivatives in order to check that the stationary points exhibit the proper number of imaginary frequencies: none for a minimum and one for a transition state (first-order saddle point). The frequency analysis results of optimized transition state show that, each transition state has only one imaginary frequency, the results: TS1 (-2009cm⁻¹), TS2 (-965cm⁻¹), TS3 (-1904 cm⁻¹), TS5 (-1752 cm⁻¹).

IRC Analysis of the Reaction

In order to verify the reaction mechanism, Intrinsic reaction coordinate (IRC) calculations were carried out to validate the connection of the reactants (CH₃OH+H₂O), transition states, intermediates, and products (HCOOH+H₂O).

The transition structure of TS1 (1C-2O-4H) was found in the study of reactions, it is a three-member ring. The TS1 link the CH₃O• and •CH₂(OH). The changes of the bond length between atoms of 1C-2O, 1C-4H and 2O-4H with the IRC curve are shown in Fig. 3.

*To whom all correspondence should be addressed.

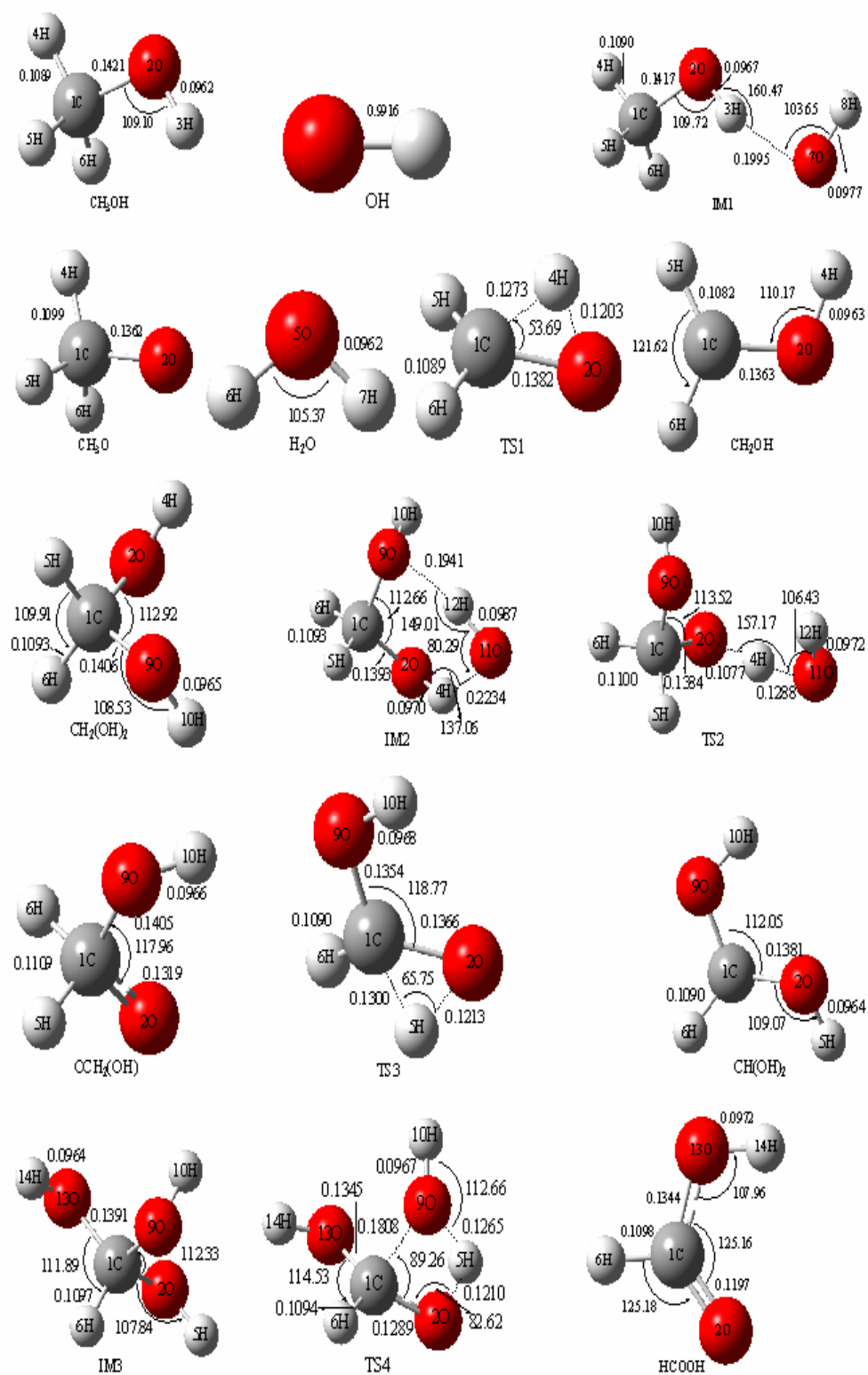


Fig. 2: The optimized geometries of the stationary points (points bond lengths are in nm, bond angles are in degree).

From the changes of bond length, the length between the 2O and 4H is significantly shortened. after the structure of transition state, the curtate trend of the length is slow down, and the 2O–4H bond appeared, The length between atoms remains unchanged; at the same time, the length of 1C–4H is greatly elongated until the bond is broken. Compared to the configuration of $\text{CH}_3\text{O}\cdot$, the length between the bond of 1C–2O of $\cdot\text{CH}_2(\text{OH})$ is slightly increased due to the 4H transferred to 2O from 1C.

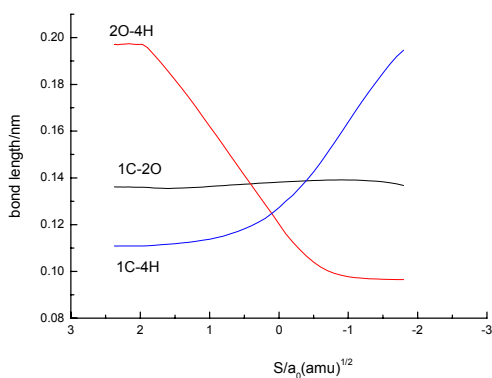


Fig. 3 Curves of bond length along Reaction path of $\text{CH}_3\text{O}\cdot \rightarrow \text{TS1} \rightarrow \cdot\text{CH}_2(\text{OH})$.

The transition structure of TS2 link the IM2 and $\cdot\text{OCH}_2(\text{OH}) + \text{H}_2\text{O}$. The 11O of $\cdot\text{OH}$ attacked the 4H (who connect with the 2O of $\text{CH}_2(\text{OH})_2$), as the 11O–4H bond appeared, the 2O–4H bond disappeared. As the $\cdot\text{OH}$ close to the $\text{CH}_2(\text{OH})_2$, there are some hydrogen bonds, and the intermediate (IM2) is formed, the results of calculation show that, the bond length of 11O–4H of IM2 is 0.2234 nm, the bond length of 12H–9O is 0.1941 nm, they are hydrogen bonds. The changes of the bond length between atoms of 11O–4H and 2O–4H with the IRC curve are shown in Fig. 4. From the changes of bond length, we can conclude that, the length between the 11O and 4H is significantly shortened. after the structure of transition state, the curtate trend of the length is slow down, and the 11O–4H bond appeared, The length between atoms remains unchanged; On the contrary, the length of 2O–4H is greatly elongated until the bond is broken.

The transition structure of TS3 (1C–2O–5H) was found in the study of reactions, it is a three-member ring. The TS3 link the $\cdot\text{OCH}_2(\text{OH})$ and $\cdot\text{CH}(\text{OH})_2$. The changes of the bond length between

atoms of 1C–2O, 1C–5H and 2O–5H with the IRC curve are shown in Fig. 5. From the changes of bond length, the length between the 2O and 5H is significantly shortened. after the structure of transition state, the curtate trend of the length is slow down, and the 2O–5H bond appeared, The length between atoms remains unchanged; at the same time, the length of 1C–5H is greatly elongated until the bond is broken. at the same time, the length between the bond of 1C–2O of $\cdot\text{CH}(\text{OH})_2$ is slightly increased compared to the configuration of $\cdot\text{OCH}_2(\text{OH})$, it is because of the 5H transfer to 2O from 1C.

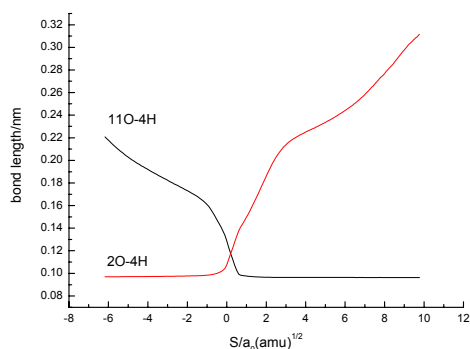


Fig. 4: Curves of bond length along Reaction path of $\text{IM2} \rightarrow \text{TS2} \rightarrow \cdot\text{OCH}_2(\text{OH}) + \text{H}_2\text{O}$.

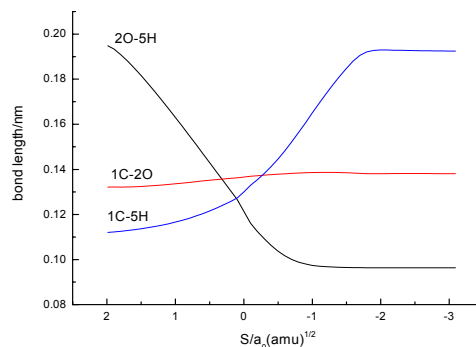


Fig. 5 Curves of bond length along Reaction path of $\cdot\text{OCH}_2(\text{OH}) \rightarrow \text{TS3} \rightarrow \cdot\text{CH}(\text{OH})_2$.

The TS4 link the IM3 and the products ($\text{HCOOH} + \text{H}_2\text{O}$). Oxygen of $\cdot\text{OH}$ attacks the carbon of $\cdot\text{CH}(\text{OH})_2$, IM3 is formed; as the closing of 9O and 5H, The transition state (TS4) structure (1C–9O–5H–2O) appeared, it is a four-member ring, changes of the bond length between atoms of 9O–5H, 2O–5H, 1C–9O and 1C–2O with the IRC curve are shown in Fig. 6. From the changes of bond length, the length

between the 9O and 5H is significantly shortened. after the structure of transition state, the curttate trend of the length is slow down, and the 9O-5H bond appeared, The length between atoms remains unchanged; On the contrary, the length of 2O-5H is greatly elongated until the bond is broken. the break about 1C-9O bond have the same trend with 2O-5H; at the same time, the length between the bond of 1C-2O of HCOOH was slightly shortened compared to the configuration of IM3, it is because of the 5H away from 2O.

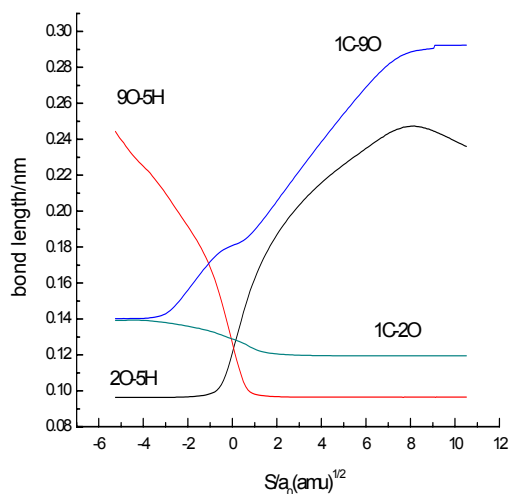


Fig. 6: Curves of bond length along Reaction path of IM3 \rightarrow TS4 \rightarrow HCOOH + H₂O.

The profile of Potential energy

The potential energy of the reactants, transition states, intermediates, and products are calculated at the B3LYP/6-311++G (2df, pd) level with thermal corrections and summarized in Table 1, and the energies are corrected by zero-point energy (ZPE) corrections. The method of B3LYP includes the exchange of energy and related gradient correction, in the past, many similar calculation of the study achieved better results [15-19], and consider of higher synthesis efficiency of this method, it's calculation time is shorter, so we adopted the results of the B3LYP methods and 6-311++G (2df, pd) basis sets.

The potential energy curves of the reactions are given in Fig. 7 and Fig. 8. The changes of Energy show that, the step of CH₃OH + •OH \rightarrow IM1 \rightarrow CH₃O• + H₂O is an exothermic process, it would release energy of 79.339184 KJ·mol⁻¹; the step of CH₃O• \rightarrow TS1 \rightarrow •CH₂(OH) needs to overcome the energy barrier of 130.870138 KJ·mol⁻¹, the step of IM2 \rightarrow TS2 \rightarrow •OCH₂(OH) + H₂O needs to overcome the energy barrier of 1.961358 KJ·mol⁻¹, the step of •OCH₂(OH) \rightarrow TS3 \rightarrow •CH(OH)₂ needs to overcome the energy barrier of 111.768554 KJ·mol⁻¹, and the step of IM3 \rightarrow TS4 \rightarrow HCOOH + H₂O needs to overcome the energy barrier of 147.884332 KJ·mol⁻¹. So it can be judged by all the steps, the barrier of the energy is lower to overcome because of the catalyzer of nano-TiO₂, it is an easy process.

Table-1: Energies for stationary points on the IRC pathways.

Species	E _{tot} ⁷ /a.u.	ΔE/(KJ·mol ⁻¹)
CH ₃ OH + •OH	-191.476243	0
IM1	-191.480875	-12.161998
CH ₃ O• + H ₂ O	-191.501828	-67.177186
CH ₃ O•	-115.061720	0
TS1	-115.011877	130.870138
•CH ₂ (OH)	-115.071538	-25.778605
CH ₂ (OH) ₂ + •OH	-266.728447	0
IM2	-266.736072	-20.020560
TS2	-266.735325	-18.059202
•OCH ₂ (OH) + H ₂ O	-266.755658	-71.446488
•OCH ₂ (OH)	-190.315547	0
TS3	-190.272979	111.768554
•CH(OH) ₂	-190.324037	-22.291745
•CH(OH) ₂ + •OH	-266.080205	0
IM3	-266.228745	-390.013648
TS4	-266.172422	-242.129316
HCOOH + H ₂ O	-266.24423	-430.671796

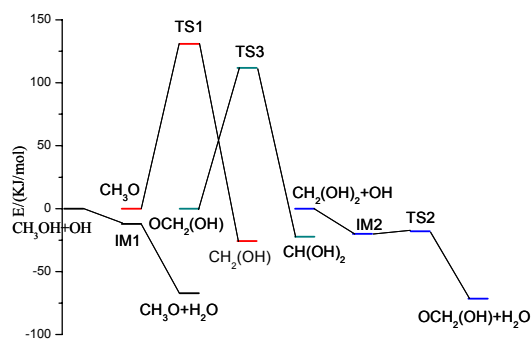


Fig.7: Relative energies of the stationary points on the reaction path of CH₃OH + •OH \rightarrow •CH(OH)₂

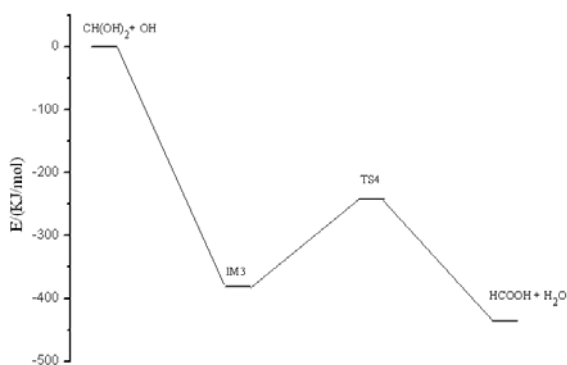


Fig. 8: Relative energies of the stationary points on the reaction path of $\bullet\text{CH}(\text{OH})_2 + \bullet\text{OH} \rightarrow \text{HCOOH} + \text{H}_2\text{O}$

Experimental

The geometries of all compounds were optimized using the hybrid density functional B3LYP with the 6-311++G (2df, pd) basis set. Harmonic vibrational frequencies calculated at the same level were used for characterization of stationary points as a minimum or a saddle point and for zero-point energy (ZPE) corrections. Transition states were subjected to intrinsic reaction coordinate (IRC) calculations to confirm the connection between reactants, intermediates, and decomposition products. All quantum calculations were performed with the Gaussian 03 program.

Conclusion

We discussed the mechanism of methanol photocatalytic degradation by nano-TiO₂, by quantum chemical method, the geometry parameters and potential energy of the reactants, transition states, intermediates, and products are calculated with quantum chemical method, and the possible reaction channels is found. The result validates the Yang's mechanism in experiment [20]; Combine with our conclusion previous [15], it predicts that the final products of methanol photocatalytic degradation are

CO₂ and H₂O. it is predicted that the potential energy surface of the channel is low, which is useful for the experiment to elimination of methanol in the air pollution.

Acknowledgements

This project was supported by the Science and technology projects of Hebei Province (Contract No. 10273939) and Handan key laboratory of organic small molecule materials, Handan College.

References

1. D. M. Baltz, E. J Chesney, M. A Tarr, A. S. Kolok and M. J. Bradley, *Transactions of the American Fisheries Society*, **134**, 730 (2005).
2. A. Becalski and K. H. Bartlett, *Indoor Air*, **16**, 153 (2006).
3. L. Chen, X. W. Zhang and L. Huang, *Chemical Engineering and Processing*, **48**, 1333 (2009).
4. D. Asensio, J. Penuelas, I. Filella and J. Llusia, *Plant and Soil*, **291**, 249 (2007).
5. J. C. Sagebiel, B. Zielinska, W. R. Pierson and A. W. Gertler, *Atmospheric Environment*, **30**, 2287 (1996).
6. P. A. Kolinko, P. G. Smirniotis, D. V. Kozlov and A. V. Vorontsov, *Journal of Photochemistry and Photobiology A: Chem.* **232**, 1 (2012).
7. J. M. Stokke and D. W. Mazyck, *Environmental Science and Technology*, **42**, 3808 (2008).
8. M. C. Li and J. N. Shen, *Journal of Solid State Electrochemistry*, **10**, 980 (2006).
9. M. I. Mejia, J. M. Marin and G. Restrepo, *Applied Catalysis. B, Environmental*, **94**, 166 (2010).
10. W. I. Kim, D. J. Suh and T. J. Park, *Topics in Catalysis*, **44**, 499 (2007).
11. E. S. Jang, S. B. Khan, J. Choi, J. Seo and H. Han, *Journal of the Chemical Society of Pakistan*, **33**, 549 (2011).
12. O. H. Birel, C. Zafer, H. Dincalp, B. Aydin and M. Can, *Journal of the Chemical Society of Pakistan*, **33**, 562 (2011).
13. Inam-Ul-Haque and M. Tariq, *Journal of the Chemical Society of Pakistan*, **33**, 529 (2011).
14. H. M. Bi, Y. Liu, F. Y. You, X. Q. Chai, P. T. Xie and J. P. Hu, *Asian Journal of Chemistry*, **24**, 1668 (2012).
15. V. Esmail, *Journal of the Chemical Society of*

- Pakistan*, **31**, 269 (2009).
16. C. Ogretir, Y. G. Sidir and I. Sidir, *Turkish Journal of Chemistry*, **34**, 977 (2010).
 17. F. Y. Liu, L. P. Meng and S. J. Zheng, *Journal of Molecula. Structure: Theochem*, **725**, 17 (2005).
 18. F. Y. Liu, L. P. Meng and S. J. Zheng, *Journal of Physics Chemical A*, **110**, 10591 (2006).
 19. L. Turker, *Journal of Molecula. Structure: Theochem*, **545**, 207 (2001).